Cell Stem Cell
Article

Regulation of Hematopoietic Stem and Progenitor Cell Mobilization by Cholesterol Efflux Pathways

Marit Westerterp,[1,2,6] Samuel Gourion-Arsiquaud,[3,4,6] Andrew J. Murphy,[1,6] Alan Shih,[5] Serge Cremers,[1] Ross L. Levine,[5] Alan R. Tall,[1,7] and Laurent Yvan-Charvet[1,7,*]
[1]Department of Medicine, Division of Molecular Medicine, Columbia University, New York, NY 10032, USA
[2]Department of Medical Biochemistry, Academic Medical Center, University of Amsterdam, Amsterdam 1105 AZ, The Netherlands
[3]Hospital for Special Surgery, New York, NY 10021, USA
[4]TRI/Princeton, Princeton, NJ 08542, USA
[5]Human Oncology and Pathogenesis Program and the Leukemia Service, Department of Medicine Memorial Sloan Kettering Cancer Center, New York, NY 10065, USA
[6]These authors contributed equally to this work
[7]These authors contributed equally to this work
*Correspondence: ly2159@columbia.edu
http://dx.doi.org/10.1016/j.stem.2012.04.024

SUMMARY

Intact cholesterol homeostasis helps to maintain hematopoietic stem and multipotential progenitor cell (HSPC) quiescence. Mice with defects in cholesterol efflux pathways due to deficiencies of the ATP binding cassette transporters ABCA1 and ABCG1 displayed a dramatic increase in HSPC mobilization and extramedullary hematopoiesis. Increased extramedullary hematopoiesis was associated with elevated serum levels of G-CSF due to generation of IL-23 by splenic macrophages and dendritic cells. This favored hematopoietic lineage decisions toward granulocytes rather than macrophages in the bone marrow leading to impaired support for osteoblasts and decreased Cxcl12/SDF-1 production by mesenchymal progenitors. Greater HSPC mobilization and extramedullary hematopoiesis were reversed by raising HDL levels in *Abca1*$^{-/-}$*Abcg1*$^{-/-}$ and *Apoe*$^{-/-}$ mice or in a mouse model of myeloproliferative neoplasm mediated by Flt3-ITD mutation. Our data identify a role of cholesterol efflux pathways in the control of HSPC mobilization. This may translate into therapeutic strategies for atherosclerosis and hematologic malignancies.

INTRODUCTION

Hematopoietic stem and multipotential progenitor cells (HSPCs) reside in specialized environments called stem cell niches in the medulla of the bone. Whereas the endosteal "osteoblastic niche" (composed of a subset of specialized osteoblasts in the inner surface of the bone cavity) is believed to maintain HSPCs in a quiescent state in poorly perfused regions, the "vascular niche" (adjacent to the bone marrow [BM] vasculature) may serve as a transit pathway that senses environmental signals and shuttles HSPCs out of the BM (Kiel et al., 2007; Lymperi et al., 2010; Ehninger and Trumpp, 2011).

In hematologic malignancies such as leukemias and myeloproliferative neoplasms, the spleen and the liver resume their fetal hematopoietic functions causing organomegaly in a process called extramedullary hematopoiesis (Kraus et al., 1998; O'Malley et al., 2005). Symptomatic splenomegaly is common and causes significant morbidity in these patients. An enlarged spleen can cause pain, early satiety, pancytopenia, portal hypertension, and hypercatabolic changes. Although not fully understood, extramedullary hematopoiesis is believed to result from conditions that disrupt the BM microenvironment, facilitating the egress of progenitor and precursor cells. Mobilization of hematopoietic stem and multipotential progenitor cells (HSPCs), mainly to the spleen, may provide a more permissive microenvironment for proliferation and myeloid differentiation (Morrison et al., 1997). Deregulation of this system contributes to the progression of myeloproliferative diseases (Perry and Li, 2007; Raaijmakers et al., 2010).

ABCA1 and ABCG1 play an important role in cholesterol homeostasis by promoting cellular cholesterol efflux to lipid-poor apoA-I and HDL particles, respectively (Wang et al., 2007; Yvan-Charvet et al., 2007). Intrinsic deficiency of these transporters in HSPCs led to expansion and proliferation of HSPCs in BM (Wang et al., 2007; Yvan-Charvet et al., 2007, 2010). However, this mechanism did not explain splenomegaly and myeloid cell infiltration of different organs observed in *Abca1*$^{-/-}$*Abcg1*$^{-/-}$ mice. An investigation of these processes led to the discovery of dramatic HSPC mobilization in *Abca1*$^{-/-}$*Abcg1*$^{-/-}$ mice reflecting increased G-CSF production. Prior studies have identified a feedback loop controlling G-CSF and neutrophil production (Stark et al., 2005). When macrophages phagocytose apoptotic neutrophils, there is suppression of production of the cytokine IL-23 leading to decreased G-CSF and neutrophil production. Our studies show that the production of IL-23 was increased in macrophages and dendritic cells deficient in ABCA1 and ABCG1 and that the resulting increase in G-CSF led to changes in the bone marrow milieu favoring release of HSPCs into the circulation.

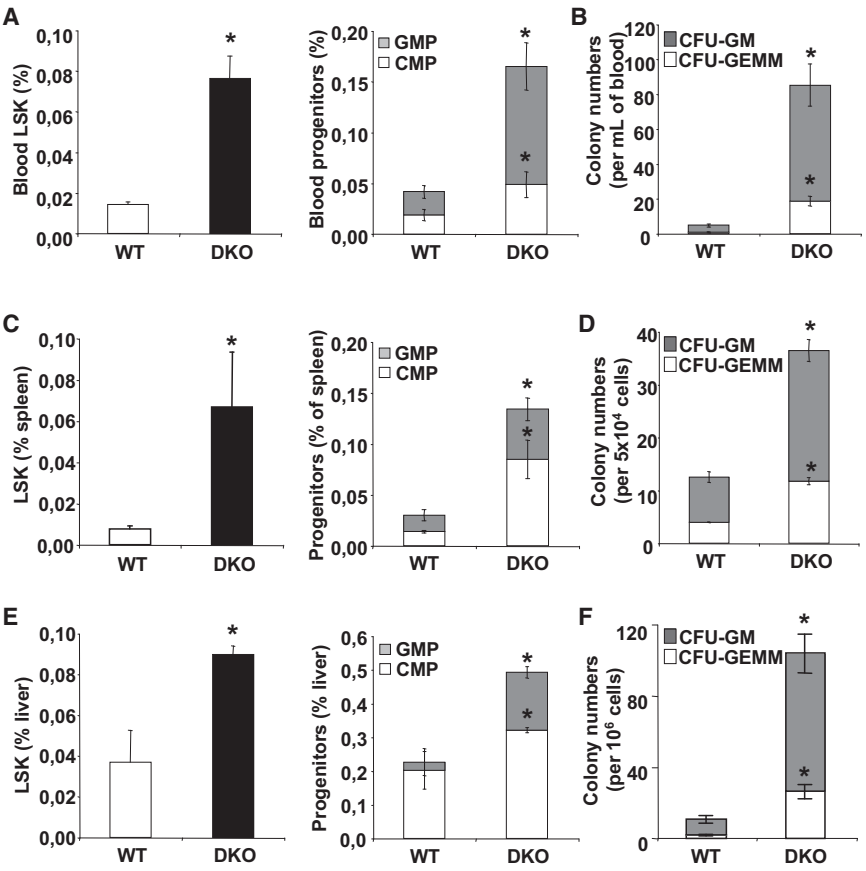

Figure 1. Extramedullary Hematopoiesis in *Abca1*$^{-/-}$*Abcg1*$^{-/-}$ Mice

Quantification of hematopoietic stem and multipotential progenitor cells (HSPCs) by flow cytometry (LSK, Lin^{-}Sca1^{+}c-Kit^{+}) or common myeloid progenitors (CMP) and granulocye/macrophage progenitors (GMP) from (A) the blood, (C) the spleen, or (E) the liver of chow fed WT and *Abca1*$^{-/-}$*Abcg1*$^{-/-}$ mice. Also displays are colony-forming unit assays of multipotential progenitors and granulocyte macrophage progenitors (CFU-GEMM and CFU-GM, respectively) from (B) the blood, (D) the spleen, or (F) the liver of chow fed WT and *Abca1*$^{-/-}$*Abcg1*$^{-/-}$ mice. Results are ± SEM of six animals per group. *$p < 0.05$ versus WT.

RESULTS

Enhanced HSPC Mobilization and Extramedullary Hematopoiesis in *Abca1*$^{-/-}$*Abcg1*$^{-/-}$ Mice

Flow cytometry analysis of HSPC, common myeloid progenitors (CMP) and granulocyte macrophage progenitors (GMP), and colony forming unit assays of multipotential progenitors (CFU-GEMM) and GMP (CFU-GM) revealed a 3-fold increase in the number of these cells in the blood of chow-fed *Abca1*$^{-/-}$*Abcg1*$^{-/-}$ mice (Figures 1A and 1B; Figure S1A available online) indicating enhanced HSPC, CMP, and GMP mobilization. Circulating LSK Flk2^{-} cells and LSK CD34^{-} cells were also proportionally increased in these mice (Figure S1B). This was associated with a parallel 3-fold increase in the number of HSPCs, CMP, and GMP progenitors and CFU-GEMM/GM in the spleen (Figures 1C, 1D, and S1D) and liver (Figures 1E, 1F, and S1E) and increased CFUs in lung and heart cell extracts (Figure S1C). These changes indicate HSPC mobilization and extramedullary hematopoiesis in multiple organs in *Abca1*$^{-/-}$*Abcg1*$^{-/-}$ mice.

BM-Dependent Regulation of HSPC Mobilization in *Abca1*$^{-/-}$*Abcg1*$^{-/-}$ Mice

Transplantation of *Abca1*$^{-/-}$*Abcg1*$^{-/-}$ BM into lethally irradiated WT recipients showed a 2-fold increase in the number of CFU in the blood of these mice while reconstitution of *Abca1*$^{-/-}$*Abcg1*$^{-/-}$ mice with WT BM reduced the number of CFU by 40% (Figure 2A). Analysis of the number of HSPCs in the spleen by flow cytometry showed parallel changes (Figure S2A). Consistent with our earlier findings, we observed that the increased number of BM LSK cells reflected a BM-dependent role of ABCA1 and ABCG1 and correlated with the cell surface expression of the IL-3Rβ on HSPCs (Figures S2B and S2C; Yvan-Charvet et al., 2010). Surprisingly, in a competitive BM transplantation experiment with equally mixed BM cells from CD45.1 WT mice and either CD45.2 WT BM or CD45.2 *Abca1*$^{-/-}$*Abcg1*$^{-/-}$ BM, we found that the mobilization of CD45.1 WT HSPCs was increased 2-fold in presence of CD45.2 *Abca1*$^{-/-}$*Abcg1*$^{-/-}$ BM cells, similar to the effect on CD45.2 *Abca1*$^{-/-}$*Abcg1*$^{-/-}$ HSPCs, suggesting that the enhanced HSPC mobilization in these mice involved a cell-extrinsic factor (Figure 2B). This was consistent with the lack of alteration in the cell-surface expression of key cytokine receptors involved in the migratory response of HSPCs in *Abca1*$^{-/-}$*Abcg1*$^{-/-}$ mice including the integrin α4β1 receptor (VLA4), the glycoprotein CD44, the stem cell growth factor receptor c-kit, and angiopoietin receptor Tie2 (Figure S2D). Cell-surface expression of CD47 in BM and peripheral HSPCs, used by these cells to hide from normal scavenging by myeloid cells (Jaiswal et al., 2009), was also unaltered in *Abca1*$^{-/-}$*Abcg1*$^{-/-}$ mice (Figure S2E). In addition, analysis of the circadian oscillation of the number of CFU showed that the appearance of HSPCs in the blood during the early phase of the diurnal cycle was increased 2.7-fold in WT recipients transplanted with *Abca1*$^{-/-}$*Abcg1*$^{-/-}$ BM compared to 1.7-fold in controls (Figure S2F). This pattern suggested that the appearance of HSPCs rather than their clearance from the blood was increased in these mice. Thus, in contrast to the cell-autonomous effect of these transporters on HSPC proliferation (Yvan-Charvet et al., 2010), HSPC mobilization in *Abca1*$^{-/-}$*Abcg1*$^{-/-}$ mice was mediated by cell-extrinsic factors.

G-CSF Dependence of HSPC Mobilization in *Abca1*$^{-/-}$*Abcg1*$^{-/-}$ BM-Transplanted Mice

We next tested the roles of IL-3, CXCL2 (or macrophage inflammatory protein, MIP2), and G-CSF, factors that were previously

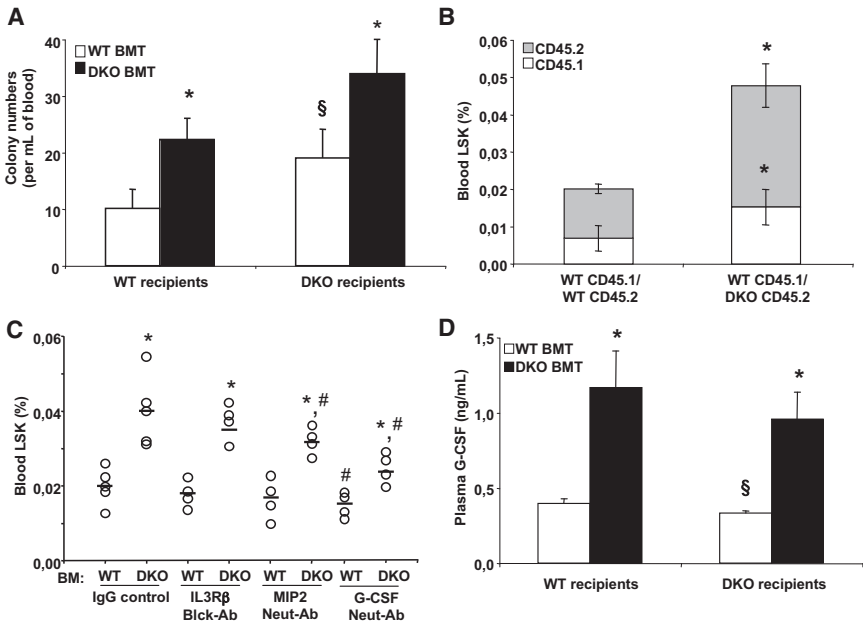

Figure 2. G-CSF-Dependence of HSPC Mobilization in *Abca1*$^{-/-}$*Abcg1*$^{-/-}$ Mice

Colony-forming unit numbers of multipotential progenitors (CFU-GEMM) from the blood of WT and *Abca1*$^{-/-}$*Abcg1*$^{-/-}$ recipient mice transplanted with either WT or *Abca1*$^{-/-}$*Abcg1*$^{-/-}$ BM 8 weeks postreconstitution (A). Competitive BM transplantation of WT CD45.1^{+} BM was equally mixed with either CD45.2^{+} WT BM or CD45.2^{+} DKO BM and transplanted into WT recipient mice. Circulating HSPCs were analyzed by flow cytometry (B). WT recipients transplanted with WT and DKO BM 14 weeks postreconstitution were i.p. injected with IgG control, 100 μg IL3Rβ blocking antibody, MIP2 (CXCL2) neutralizing antibody, or G-CSF neutralizing antibody for 16 hr and analyzed for circulating HSPCs (C). Plasma G-CSF levels in WT and *Abca1*$^{-/-}$*Abcg1*$^{-/-}$ recipient mice transplanted with either WT or *Abca1*$^{-/-}$*Abcg1*$^{-/-}$ BM 8 weeks postreconstitution are shown (D). Results are ± SEM of five or six animals per group. *$p < 0.05$ versus WT recipients transplanted with WT BM. $^{\#}p < 0.05$ versus IgG control. $^{\S}p < 0.05$ versus *Abca1*$^{-/-}$*Abcg1*$^{-/-}$ recipients transplanted with *Abca1*$^{-/-}$*Abcg1*$^{-/-}$ BM.

shown to be increased in *Abca1*$^{-/-}$*Abcg1*$^{-/-}$ mice (Yvan-Charvet et al., 2007, 2008) and also known to have key roles in the regulation of HSPC mobilization (Guillaume et al., 1993; Fibbe et al., 1999; Metcalf, 2008; Greenbaum and Link, 2011). Although injection of IL-3Rβ or CXCL2 blocking antibodies did not prevent the enhanced HSPC mobilization of WT recipients transplanted with *Abca1*$^{-/-}$*Abcg1*$^{-/-}$ BM, the G-CSF neutralizing antibody caused a major reduction in the mobilization of HSPCs in these mice (Figure 2C) and in the number of HSPCs in the spleen (data not shown). Alteration in the expression of the G-CSF receptor was unlikely to explain these effects because there was no significant change in its cell-surface expression or mRNA level in different BM populations of *Abca1*$^{-/-}$*Abcg1*$^{-/-}$ mice (Figures S3A–S3C). Consistent with a lack of expression of G-CSF receptor on HSPCs (Liu et al., 2000), addition of G-CSF to in vitro BM cultures did not promote expansion of either WT or *Abca1*$^{-/-}$*Abcg1*$^{-/-}$ HSPCs (Figure S3D), and the G-CSF neutralizing antibody did not modulate the number of BM HSPC in these mice (Figure S3E). The increased plasma G-CSF in *Abca1*$^{-/-}$*Abcg1*$^{-/-}$ mice was a BM-mediated effect (Figure 2D). Thus, the absence of ABCA1 and ABCG1 in myeloid BM-derived cells led to an increase in plasma G-CSF that in turn caused increased mobilization of HSPCs.

Increased IL-23/IL-17 Drives G-CSF-Dependent HSPC Mobilization in *Abca1*$^{-/-}$*Abcg1*$^{-/-}$ BM-Transplanted Mice

Consistent with the central role of interleukin-17 (IL-17) as a potent inducer of G-CSF (Fossiez et al., 1996), we found increased plasma IL-17 levels in *Abca1*$^{-/-}$*Abcg1*$^{-/-}$ BM-transplanted mice (Figure 3A). We also showed that the administration of an IL-17 blocking antibody was able to normalize both plasma G-CSF levels (Figure 3B) and CFU numbers (Figure 3C) in WT recipients transplanted with *Abca1*$^{-/-}$*Abcg1*$^{-/-}$ BM. The production of IL-17 can be mediated by commensal bacteria from the intestinal flora (Ivanov et al., 2008) or by the secretion of interleukin-23 (IL-23) from splenic phagocytic cells (Stark et al., 2005). Despite hypertrophy of intestinal Peyer's patches in *Abca1*$^{-/-}$*Abcg1*$^{-/-}$ mice (Yvan-Charvet et al., 2010), treatment of these mice with broad spectrum antibiotics including vancomycin (Yvan-Charvet et al., 2010) to suppress segmented filament bacteria involved in the induction of intestinal Th17 (Ivanov et al., 2008) did not reduce their plasma IL-17 or G-CSF levels (Figures 3D and S3F). In contrast, we found a 4-fold increase in IL-23 concentration in the spleen of these mice, an effect that was dependent on the absence of ABCA1 and ABCG1 in BM-derived myeloid cells (Figure 3E). Treatment with an IL-23R neutralizing antibody reduced both plasma IL-17 and G-CSF levels in WT recipients transplanted with *Abca1*$^{-/-}$*Abcg1*$^{-/-}$ BM (Figures 3F and S3G) and also the number of CFU in the blood (Figure S3H).

ABCA1 and ABCG1 Deficiency in Macrophages and Dendritic Cells Promotes HSPC Mobilization

Because IL-23 is secreted by phagocytic macrophages and dendritic cells (Stark et al., 2005), we generated macrophage-specific ABCA1/ABCGG1 knockouts (*LysM-cre Abca1*$^{fl/fl}$*Abcg1*$^{fl/fl}$) and dendritic cell-specific ABCA1/ABCG1 knockouts (*CD11c-cre Abca1*$^{fl/fl}$*Abcg1*$^{fl/fl}$) to examine the contribution of these cells to HSPC mobilization. *LysM-cre Abca1*$^{fl/fl}$*Abcg1*$^{fl/fl}$ and *CD11c-cre Abca1*$^{fl/fl}$*Abcg1*$^{fl/fl}$ mice showed >95% reductions in ABCA1/ABCG1 expression in macrophages and dendritic cells, respectively, and no difference in ABCA1/ABCG1 expression in HSPCs (data not shown). We observed that *LysM-cre Abca1*$^{fl/fl}$*Abcg1*$^{fl/fl}$ and *CD11c-cre Abca1*$^{fl/fl}$*Abcg1*$^{fl/fl}$ mice exhibited a 1.5-fold and 1.8-fold increase in IL-23 content in their spleen compared to their respective controls (Figure 4A), with a parallel increase in the number of CFU in the blood (Figure 4B). This was also associated with an increase in plasma IL-17 (Figure 4C) and G-CSF (Figure 4D) levels. In vitro experiments showed that IL-23 mRNA levels were increased in *LysM-cre Abca1*$^{fl/fl}$*Abcg1*$^{fl/fl}$ macrophages

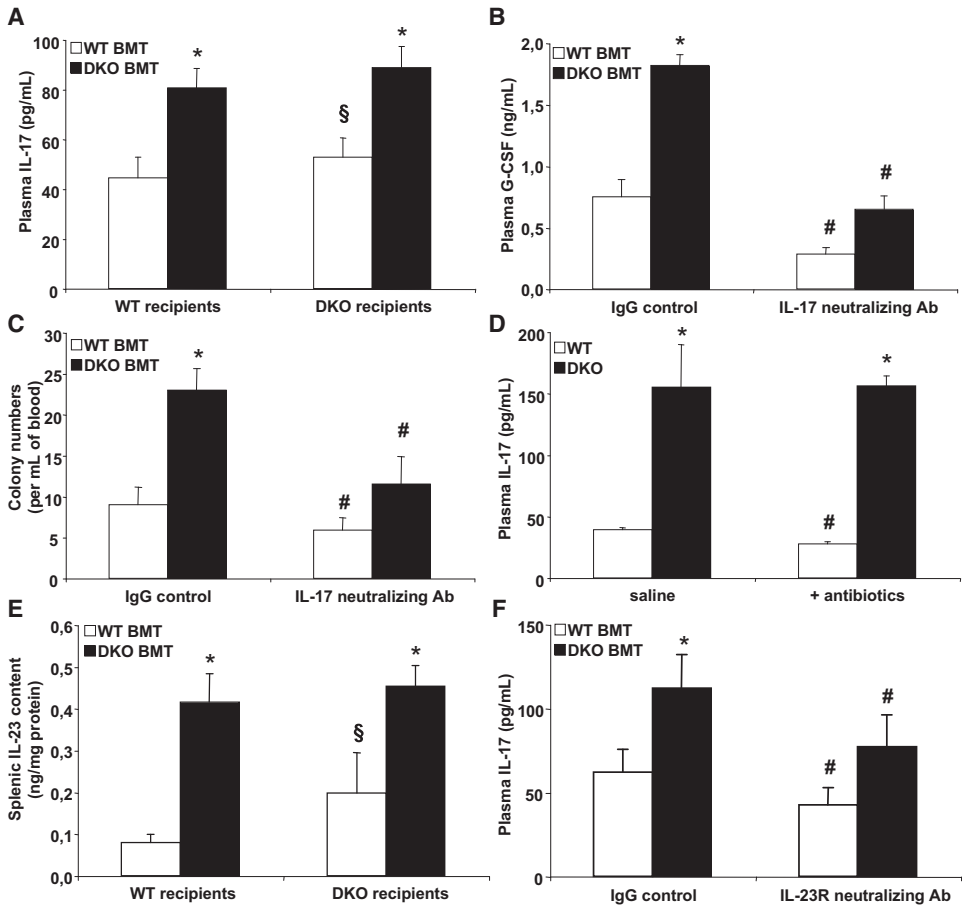

Figure 3. IL-23/IL-17-Dependent G-CSF Regulation in *Abca1*$^{-/-}$*Abcg1*$^{-/-}$ Mice

Plasma IL-17 levels in WT and *Abca1*$^{-/-}$*Abcg1*$^{-/-}$ recipient mice transplanted with either WT or *Abca1*$^{-/-}$*Abcg1*$^{-/-}$ BM 8 weeks postreconstitution (A). Plasma G-CSF levels in WT recipients transplanted with WT and *Abca1*$^{-/-}$*Abcg1*$^{-/-}$ BM 14 weeks postreconstitution and i.p. injected with IgG control or 250 μg IL-17 neutralizing antibody for 16 hr are shown (B). Colony-forming unit numbers from the blood of these mice are displayed in (C). Plasma IL-17 levels in WT and *Abca1*$^{-/-}$*Abcg1*$^{-/-}$ mice treated with broad-spectrum antibiotics for 2 weeks to deplete commensal bacteria are shown in (D). IL-23 protein content in the spleen of WT and *Abca1*$^{-/-}$*Abcg1*$^{-/-}$ recipient mice transplanted with either WT or *Abca1*$^{-/-}$*Abcg1*$^{-/-}$ BM 8 weeks postreconstitution is shown in (E). Plasma IL-17 levels in WT recipients transplanted with WT and *Abca1*$^{-/-}$*Abcg1*$^{-/-}$ BM 14 weeks postreconstitution and i.p. injected with IgG control or 200 μg IL-23R neutralizing antibody for 16 hr are illustrated in (F). Results are ± SEM of five or six animals per group. *$p < 0.05$ versus WT recipients transplanted with WT BM. #$p < 0.05$ versus IgG control. §$p < 0.05$ versus *Abca1*$^{-/-}$*Abcg1*$^{-/-}$ recipients transplanted with *Abca1*$^{-/-}$*Abcg1*$^{-/-}$ BM.

and *CD11c-cre Abca1*$^{fl/fl}$*Abcg1*$^{fl/fl}$ dendritic cells under steady state or LPS- and poly(I:C)-stimulated conditions (Figure 4E). In addition, plasma membrane cholesterol depletion by cyclodextrin significantly reduced the mRNA expression levels of IL-23 in *LysM-cre Abca1*$^{fl/fl}$*Abcg1*$^{fl/fl}$ macrophages under steady state or LPS- and poly(I:C)-stimulated conditions (Figure 4E) and completely reversed the increase in *CD11c-cre Abca1*$^{fl/fl}$ *Abcg1*$^{fl/fl}$ dendritic cells (Figure 4F). Thus, in addition to its known role in promoting granulopoiesis (Stark et al., 2005), IL-23/IL-17/G-CSF signaling is now shown to be associated with enhanced HSPC mobilization. Cholesterol efflux pathways in macrophages and dendritic cells suppressed this signaling pathway.

Increased proteolytic cleavage of CXCR4 in *Abca1*$^{-/-}$*Abcg1*$^{-/-}$ HSPCs is not sufficient to promote their mobilization. These experiments have been described in the Supplemental Experimental Procedures available online.

Decreased Cxcl12 Expression in BM of *Abca1*$^{-/-}$*Abcg1*$^{-/-}$ Mice due to Decreased Expression in Osteoblasts and Nestin^{+} Progenitors

These observations suggested that an alternative pathway was involved in the enhanced HSPC mobilization of *Abca1*$^{-/-}$ *Abcg1*$^{-/-}$ mice. Recent evidence suggests that G-CSF may decrease Cxcl12/SDF-1 expression (Semerad et al., 2005). Cxcl12/SDF-1 was reduced by 25% in BM fluid of WT recipients transplanted with *Abca1*$^{-/-}$*Abcg1*$^{-/-}$ BM, with or without CXCR4 lentiviral overexpression (Figure S4J). There was a 50% decrease in Cxcl12/SDF-1 mRNA expression and protein content in the BM (Figure S5A). As the number of dipeptidyl peptidase-4 (CD26/DPPIV)-positive cells measured by flow cytometry was reduced by 60% in *Abca1*$^{-/-}$*Abcg1*$^{-/-}$ BM (Figure S5B), this suggested that the altered production rather than the cleavage of Cxcl12/SDF-1 was impaired in these mice. Consistent with this observation, the number of

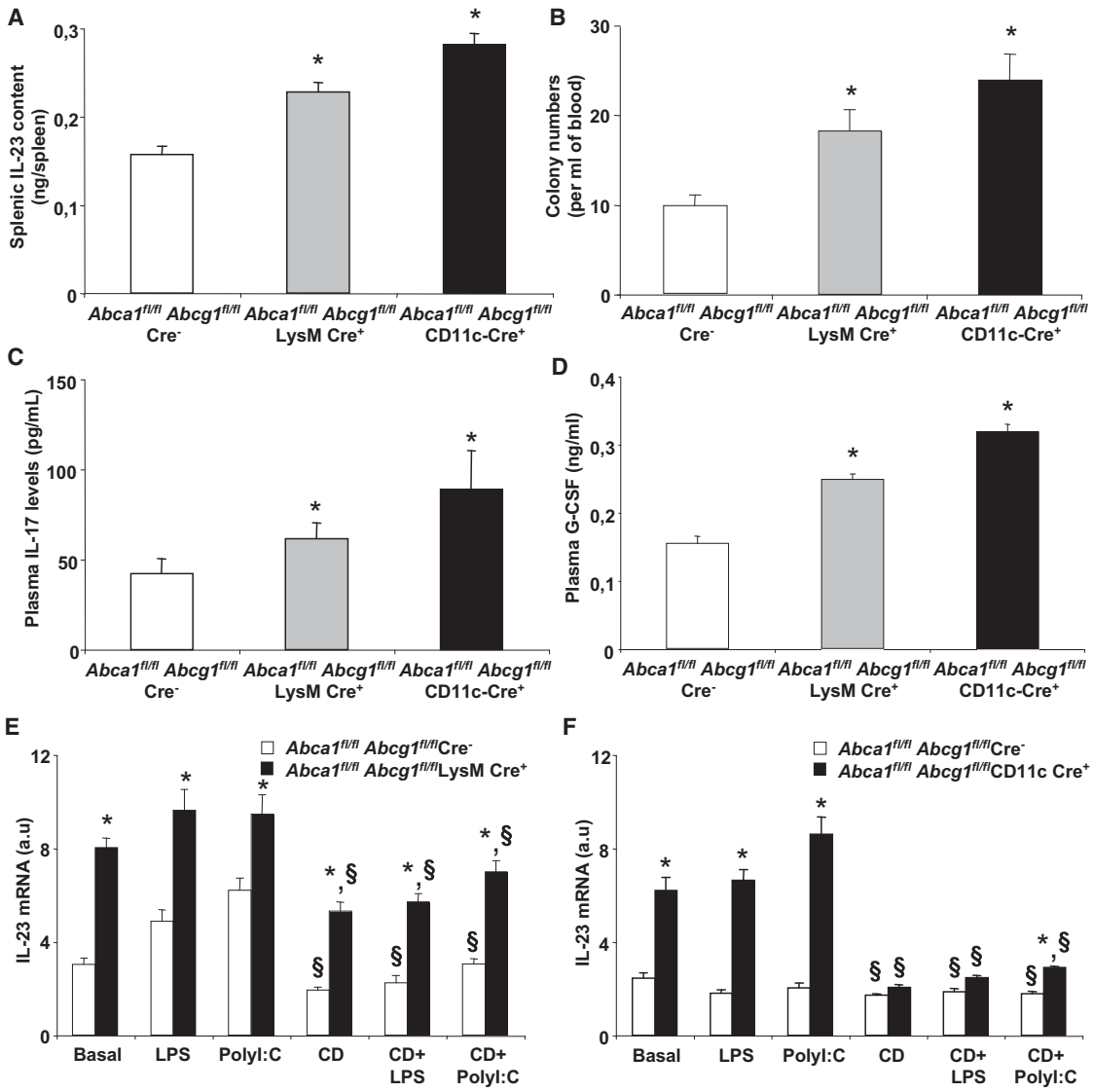

Figure 4. Deficiency of ABCA1 and ABCG1 in Macrophages and Dendritic Cells Promotes the G-CSF-Dependent HSPC Mobilization

Splenic IL-23 protein content (A), colony-forming unit numbers (B), plasma G-CSF levels (C), and plasma IL-17 levels (D) in 28-week-old *Abca1*$^{fl/fl}$*Abcg1*$^{fl/fl}$ (controls), *LysM-Cre Abca1*$^{fl/fl}$*Abcg1*$^{fl/fl}$, and *CD11c-Cre Abca1*$^{fl/fl}$*Abcg1*$^{fl/fl}$ mice. Results are ± SEM of five or six animals per group. *p < 0.05 versus controls. Modulation of IL-23 mRNA expression levels in *Abca1*$^{fl/fl}$*Abcg1*$^{fl/fl}$ and *LysM-Cre Abca1*$^{fl/fl-}$*Abcg1*$^{fl/fl}$ BM-derived macrophages (E) and *CD11c-Cre Abca1*$^{fl/fl}$ *Abcg1*$^{fl/fl}$ BM-derived dendritic cells (F) are shown after manipulation of plasma membrane cholesterol. Cells were incubated with 5 mmol/l cyclodextrin (CD) for 30 min before treatment with 50 ng/ml lipopolysaccharide (LPS, TLR4 ligand) or 2.5 μg/ml Polyl:C (TLR3 ligand) for 3 hr. IL-23 transcript levels were normalized to m36B4 mRNA amount. RNA levels were expressed as arbitrary units (a.u.). Values are mean ± SEM of an experiment performed in quadruplicate. *p < 0.05 versus respective controls. §p < 0.05 versus conditions without cyclodextrin treatment.

SDF-1-expressing reticular (CAR) cells (Sugiyama et al., 2006) but not non-SDF-1-expressing cells was reduced in *Abca1*$^{-/-}$ *Abcg1*$^{-/-}$ BM (Figure S5C). Together these findings suggested that the enhanced HSPC mobilization of *Abca1*$^{-/-}$*Abcg1*$^{-/-}$ BM-transplanted mice could not be attributed to increased neutrophil elastase 2-dependent CXCR4 cleavage but rather reflected reduced *SDF-1/Cxcl12* mRNA expression. In addition, we found that the 50% decrease in SDF-1/Cxcl12 BM fluid content was mainly attributable to the lack of ABCA1 and ABCG1 in BM-derived myeloid cells (Figure 5A). Endothelial cells, osteoblasts (OBs), and Nestin^{+} mesenchymal stem cells (MSCs) were reported to be the major Cxcl12/SDF-1-expressing cell types within the BM (Dar et al., 2005; Semerad et al., 2005; Christopher et al., 2009; Méndez-Ferrer et al., 2010). To gain more insight into the regulation of Cxcl12/SDF-1 in *Abca1*$^{-/-}$ *Abcg1*$^{-/-}$ mice, we bred these mice with mice expressing yellow fluorescent protein (YFP) under the control of regulatory elements of the nestin promoter to allow the identification of Nestin^{+} MSCs. We compared the mRNA expression levels of Cxcl12/SDF-1 in sorted CD45-Ter119^{-}Nestin^{+} MSCs, Lin^{-} CD45^{-}CD31^{-}Sca-1^{-}CD51^{+} OB lineage cells, and Lin^{-}CD45^{-} CD31^{+} endothelial cells (Figure S5D). High osteocalcin and

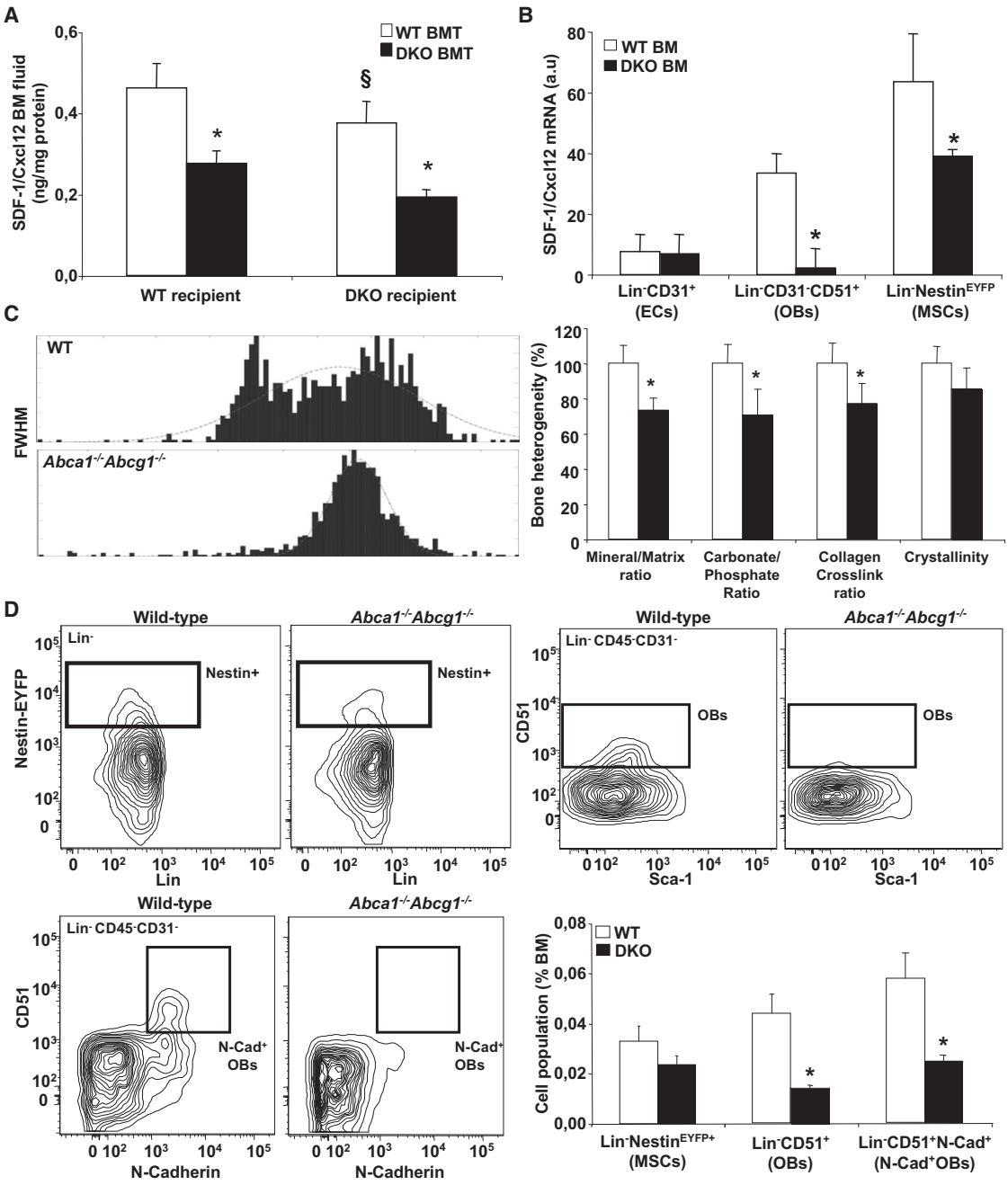

Figure 5. Reduced Osteoblastic SDF-1/Cxcl12 Production in *Abca1*$^{-/-}$*Abcg1*$^{-/-}$ Mice

Quantification of the SDF-1/Cxcl12 protein content in the BM fluid of WT and *Abca1*$^{-/-}$*Abcg1*$^{-/-}$ recipient mice transplanted with either WT or *Abca1*$^{-/-}$*Abcg1*$^{-/-}$ BM 8 weeks postreconstitution (A). *SDF-1/Cxcl12* mRNA levels normalized to ribosomal m36B4 in sorted Lin$^-$CD45$^-$CD31$^+$ endothelial cells (ECs), Lin$^-$CD45$^-$CD31$^-$Sca1$^-$CD51$^+$ OB lineage cells (OBs), and Lin-Nestin$^+$ progenitors (MSCs) from Nestin-Cre$^+$Gt(Rosa)26^{Sor} and *Abca1*$^{-/-}$*Abcg1*$^{-/-}$ Nestin-Cre$^+$Gt(Rosa)26^{Sor} mice are shown in (B). Representative histograms and percentage changes in the bone heterogeneity of the indicated bone mineral and matrix properties quantified by Fourier Transform Infrared (FTIR) spectroscopy as the full width at half maximum (FWHM) of the pixel histogram distribution (PHD) are shown in (C). Representative dot plots and quantification of Lin-Nestin$^+$ MSCs, Lin$^-$CD45$^-$CD31$^-$Sca1$^-$CD51$^+$ OB lineage cells, and Lin$^-$CD45$^-$CD31$^-$CD51$^+$N-Cadherin$^+$ OBs by flow cytometry are displayed in (D). Results are ± SEM of five or six animals per group. *$p < 0.05$ versus WT. §$p < 0.05$ versus *Abca1*$^{-/-}$*Abcg1*$^{-/-}$ recipients transplanted with *Abca1*$^{-/-}$*Abcg1*$^{-/-}$ BM.

VE-cadherin expression confirmed that bone Lin$^-$CD45$^-$CD31$^-$Sca-1$^-$CD51$^+$ cells and Lin$^-$CD45$^-$CD31$^+$ cells were enriched in OBs and endothelial cells, respectively (Figure S5E). As previously reported, BM endothelial cells expressed low amount of Cxcl12/SDF-1 compared to OBs (Semerad et al., 2005), and no change was observed between WT and *Abca1*$^{-/-}$*Abcg1*$^{-/-}$ mice (Figure 5B). Although ABCA1 and ABCG1 mRNA expression were barely detectable in Nestin$^+$ MSCs and OBs

(data not shown), there was a 50% decrease in Cxcl12/SDF-1 expression in Nestin$^+$ MSCs and almost complete absence of Cxcl12/SDF-1 expression in OBs isolated from *Abca1*$^{-/-}$*Abcg1*$^{-/-}$ BM compared to controls (Figure 5B). Vascular cell adhesion molecule-1 (VCAM-1), another HSPC maintenance gene, was also reduced in these cells (data not shown). Thus, lack of ABCA1 and ABCG1 indirectly modulates the expression of the key HSPC maintenance gene Cxcl12/SDF-1 in OBs and their Nestin$^+$ progenitors.

Reduced Cxcl12/SDF-1 Expression in *Abca1*$^{-/-}$*Abcg1*$^{-/-}$ BM Is Associated with Decreased N-Cadherin$^+$ Osteoblasts

In addition to reduced Cxcl12/SDF-1 expression in OBs and their Nestin$^+$ progenitors, it has been shown that reduced osteoblast numbers, especially N-Cadherin$^+$ bone-lining, spindle-shaped OBs, could contribute to the lack of HSPC retention within the BM (Zhang et al., 2003; Visnjic et al., 2004; Lymperi et al., 2008). Bone histomorphometry analysis in *Abca1*$^{-/-}$*Abcg1*$^{-/-}$ mice revealed no significant change in the percentage of bone cancellous surface occupied by various heterogeneous populations of OBs including endosteal, trabecular, and periosteal OBs as well as osteoclasts (Figure S5F). These data were consistent with similar bone mineral density measured in vivo by DEXA (Figure S5G). Fourier transform infrared imaging (FTIRI) analysis of tibial cortical bone also revealed similar mineral/matrix, carbonate/phosphate and collagen crosslink ratio, as well as crystallinity between WT and *Abca1*$^{-/-}$*Abcg1*$^{-/-}$ mice (Figure S5H). Thus, the enhanced HSPC mobilization in *Abca1*$^{-/-}$*Abcg1*$^{-/-}$ mice was not the consequence of altered mineral or matrix bone properties. However, a decrease in the heterogeneous distribution of bone tissue material properties was noted for almost all of the measured FTIRI parameters in the bone of *Abca1*$^{-/-}$*Abcg1*$^{-/-}$ mice (Figure 5C). This reflected reduced bone remodeling with fewer regions of newly formed bone tissue (Gourion-Arsiquaud et al., 2010) and suggested some specificity in osteoblastic lineage fate in these mice. Although the reduced number of Nestin$^+$ MSCs in *Abca1*$^{-/-}$*Abcg1*$^{-/-}$ BM did not reach significance (Figure 5D), there was a pronounced 3-fold decrease in the number of Lin$^-$CD45$^-$CD31$^-$Sca-1$^-$CD51$^+$ OB lineage cells (Figure 5D). We also observed similar reductions in Lin$^-$CD45$^-$CD31$^-$CD51$^+$N-Cadherin$^+$ OB population in the BM of these mice (Figure 5D). Of note, all Lin$^-$CD45$^-$CD31$^-$CD51$^+$Sca-1$^-$ OBs were N-Cadherin$^+$ (data not shown). Thus, the reduced production of SDF-1/Cxcl12 in *Abca1*$^{-/-}$*Abcg1*$^{-/-}$ BM reflected not only reduced expression of this HSPC maintenance gene but also decreased numbers of N-Cadherin$^+$ OB-derived Nestin$^+$ MSCs.

Depletion of BM Macrophages Contributes to Reduced Cxcl12/SDF-1 Expression in *Abca1*$^{-/-}$*Abcg1*$^{-/-}$ BM

Recent studies have highlighted a role of BM macrophages in supporting osteoblast differentiation and SDF-1/Cxcl12 production (Winkler et al., 2010; Christopher et al., 2011; Chow et al., 2011). We next examined BM macrophages by flow cytometry in WT and *Abca1*$^{-/-}$*Abcg1*$^{-/-}$ mice transplanted with either WT or *Abca1*$^{-/-}$*Abcg1*$^{-/-}$ BM. Two different populations of macrophages have been described in the BM, namely CD11b^{hi} osteomacs (Winkler et al., 2010) and CD11b^{int}CD169$^+$ macrophages (Chow et al., 2011) that are localized in different hypoxic area of the BM (Ehninger and Trumpp, 2011). The gating strategy is provided in Figure S6A. Both populations of macrophages were dramatically reduced, by 2- and 4-fold, respectively, in WT recipients transplanted with *Abca1*$^{-/-}$*Abcg1*$^{-/-}$ BM, and this was dependent on a role of ABCA1 and ABCG1 within the BM-derived myeloid population as shown by the fact that transplantation of WT BM into *Abca1*$^{-/-}$*Abcg1*$^{-/-}$ recipients almost completely reversed this loss (Figures 6A and 6B). Interestingly, the role of G-CSF in mediating HSPC mobilization was recently shown to involve the G-CSF receptor within cells of the monocytic lineage (Christopher et al., 2011). Therefore, we next took advantage of the finding that the IL-17 neutralizing antibody reduced the plasma G-CSF levels in these mice. Treatment of WT recipients transplanted with *Abca1*$^{-/-}$*Abcg1*$^{-/-}$ BM with this antibody largely rescued the loss of both BM macrophage populations (Figures 6C and 6D) and the reduced SDF-1/Cxcl12 BM fluid content (Figure S6B). Similar findings were observed with the use of IL-23R neutralizing antibody (Figures S6C and S6D) and reduced BM macrophage populations were also observed in *LysM-cre Abca1*$^{fl/fl}$*Abcg1*$^{fl/fl}$ and *CD11c-cre Abca1*$^{fl/fl}$*Abcg1*$^{fl/fl}$ mice (Figure S6E). This revealed that the enhanced IL-23/IL-17/G-CSF axis contributed substantially to the depletion of both BM macrophage populations and subsequent loss of BM SDF-1/Cxcl12 production. Finally, consistent with earlier work (Zhu and Emerson, 2002; Rieger et al., 2009), in vitro BM cultures showed that G-CSF treatment of *Abca1*$^{-/-}$*Abcg1*$^{-/-}$ BM cultures resulted in increased neutrophil but decreased monocyte production, whereas IL-3 treatment increased both neutrophils and monocytes, suggesting that G-CSF instructed hematopoietic progenitor determination to favor neutrophilic over monocytic lineages (Figures S6F and S6G). Consistent with these findings, we observed that in vitro treatment of WT BM cells with 10% serum from *Abca1*$^{-/-}$*Abcg1*$^{-/-}$ mice favored mainly GMP and to some extent MDP expansion compared to WT serum (Figures 6E, S6H, and S6I), leading to a major increase in the number of neutrophils (Figure 6F). The use of the G-CSF neutralizing antibody in these cultures revealed that the inhibition of GMP and neutrophil expansion (Figures 6E and 6F) was associated with a significant increase in the number of monocytes (Figure 6F), indicating that G-CSF acted at the level of GMP to tightly control the leukocyte fate. Thus, we propose that enhanced IL-23/IL-17-dependent G-CSF production by *Abca1*$^{-/-}$*Abcg1*$^{-/-}$ splenic phagocytic cells induced HSPC mobilization by altering the fate of GMPs such that there was decreased formation of monocyte/macrophage-lineage cells and decreased macrophage-dependent osteoblastic support and SDF-1/Cxcl12 production.

Raising HDL-Cholesterol Suppresses HSPC Mobilization in Mouse Models of Hypercholesterolemia and Myeloproliferative Disorders

Expression of the human apoA-I transgene led to reduced plasma G-CSF (Figure 7A) and reduced HSPC mobilization in *Abca1*$^{-/-}$*Abcg1*$^{-/-}$ BMT mice (Figure 7B), providing a mechanism to explain the reversal of extramedullary hematopoiesis, splenomegaly, and myeloid cell proliferation by the apoA-I transgene. This was associated with reduced splenic mRNA expression of IL-23 (data not shown). We next tested whether the

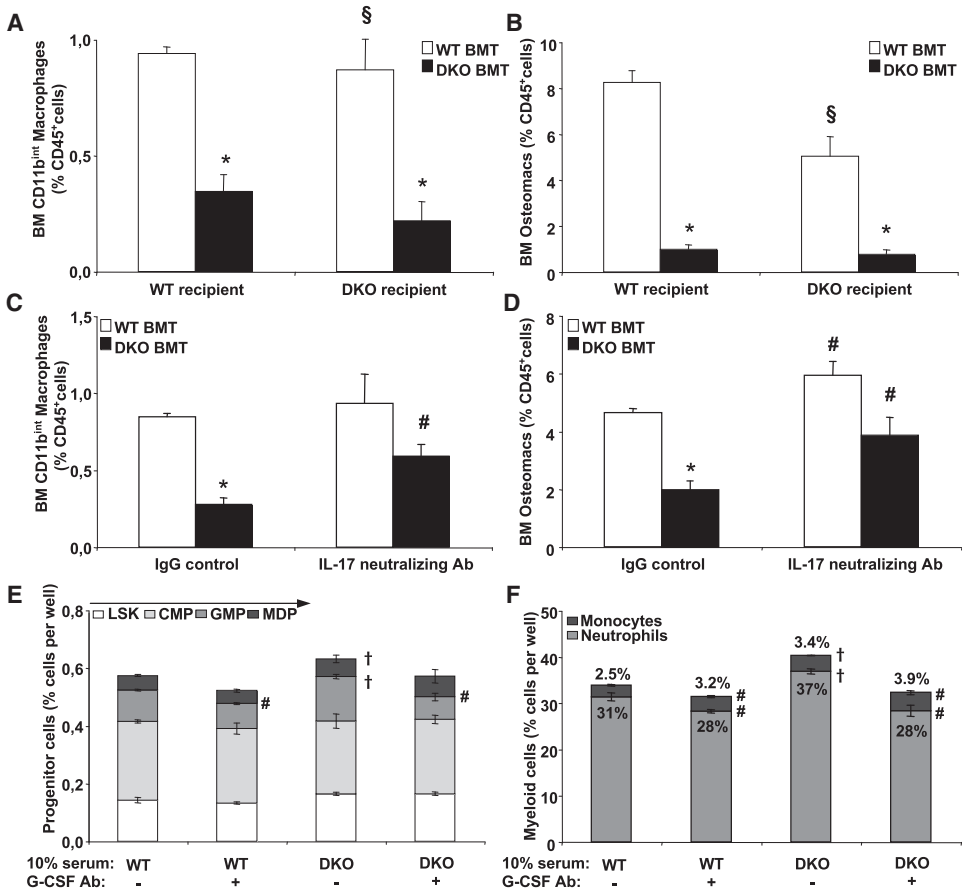

Figure 6. Depletion of BM Macrophages in *Abca1*$^{-/-}$*Abcg1*$^{-/-}$ Mice

Quantification of BM macrophage subsets by flow cytometry in WT and *Abca1*$^{-/-}$*Abcg1*$^{-/-}$ recipient mice transplanted with either WT or *Abca1*$^{-/-}$*Abcg1*$^{-/-}$ BM 8 weeks postreconstitution (A and B) and in WT recipients transplanted with WT and *Abca1*$^{-/-}$*Abcg1*$^{-/-}$ BM 14 weeks postreconstitution and i.p. injected with IgG control or 250 μg IL-17 neutralizing antibody for 16 hr (C and D). Results are ± SEM of five or six animals per group. *$p < 0.05$ versus WT. §$p < 0.05$ versus *Abca1*$^{-/-}$*Abcg1*$^{-/-}$ recipients transplanted with *Abca1*$^{-/-}$*Abcg1*$^{-/-}$ BM. Quantification of hematopoietic progenitors (E), monocytes, and neutrophils (F) in WT BM cultures grown for 48 hr in liquid culture in presence of 10% of the indicated serum and 50 ng/mL G-CSF neutralizing antibody (+) or control non-specific IgG (–) are shown. Results are ± SEM of three independent experiments. #$p < 0.05$ versus IgG control. †$p < 0.05$ versus 10% WT serum.

suppression of HSPC mobilization by raising HDL levels in *Abca1*$^{-/-}$*Abcg1*$^{-/-}$ BM-transplanted mice was peculiar to this model or could be observed as a more general phenomenon in other mouse models of hypercholesterolemia or MPN. We recently reported that hypercholesterolemic *Apoe*$^{-/-}$ mice exhibited a similar phenotype to *Abca1*$^{-/-}$*Abcg1*$^{-/-}$ mice and that infusion of rHDL suppressed their leukocytosis (Murphy et al., 2011). *Apoe*$^{-/-}$ mice fed a high fat diet for 4 weeks exhibited a 2-fold increased plasma G-CSF levels (Figure 7C) that correlated with their number of circulating HSPCs (Figure 7D). Infusion of 80 mg/kg rHDL reduced by approximately 40% not only the plasma G-CSF levels (Figure 7C) but also the number of circulating HSPCs in these mice 96 hr postinfusion (Figure 7D). Finally, we transplanted BM transduced with retroviruses encoding Flt3-ITD, an oncogenic mutation previously identified in acute myeloid leukemia (AML) that confers a fully penetrant myeloproliferative disorder in mice (Kelly et al., 2002) into either WT or apoA-I transgenic mice. Reduced plasma HDL-cholesterol levels have been previously reported in myeloproliferative disorders (Gilbert et al., 1981; Dessì et al., 1995). Consistent with these reports, mice bearing the Flt3-ITD mutation exhibited a 1.5-fold decrease in their plasma HDL-cholesterol levels (Figure S7A) and this was associated with reduced mRNA expression levels of ABCA1 but not ABCG1 in their spleen (Figure S7B). Remarkably, there was a 4-fold increase in plasma G-CSF levels and circulating HSPC numbers in mice bearing the Flt3-ITD mutation, and both parameters were markedly reduced by the human apoA-I transgene (Figures 7E and 7F). This was associated with reduced mRNA expression of IL-23 in their spleen (Figure S7C), reduced plasma IL-17 (Figure S7D), and suppression of splenomegaly (Figure S7E) and splenic HSPC infiltration (Figure S7F). Finally, the depletion of HSPCs in the BM of mice bearing the Flt3-ITD mutation was prevented by overexpression of the apoA-I transgene (Figure S7G), reflecting increased mRNA expression levels of SDF-1/Cxcl12 (Figure S7H). Thus, similar mechanisms of HSPC mobilization and reversal by increased HDL levels appear to be involved in both the *Abca1*$^{-/-}$*Abcg1*$^{-/-}$ and the Flt3-ITD models of MPNs.

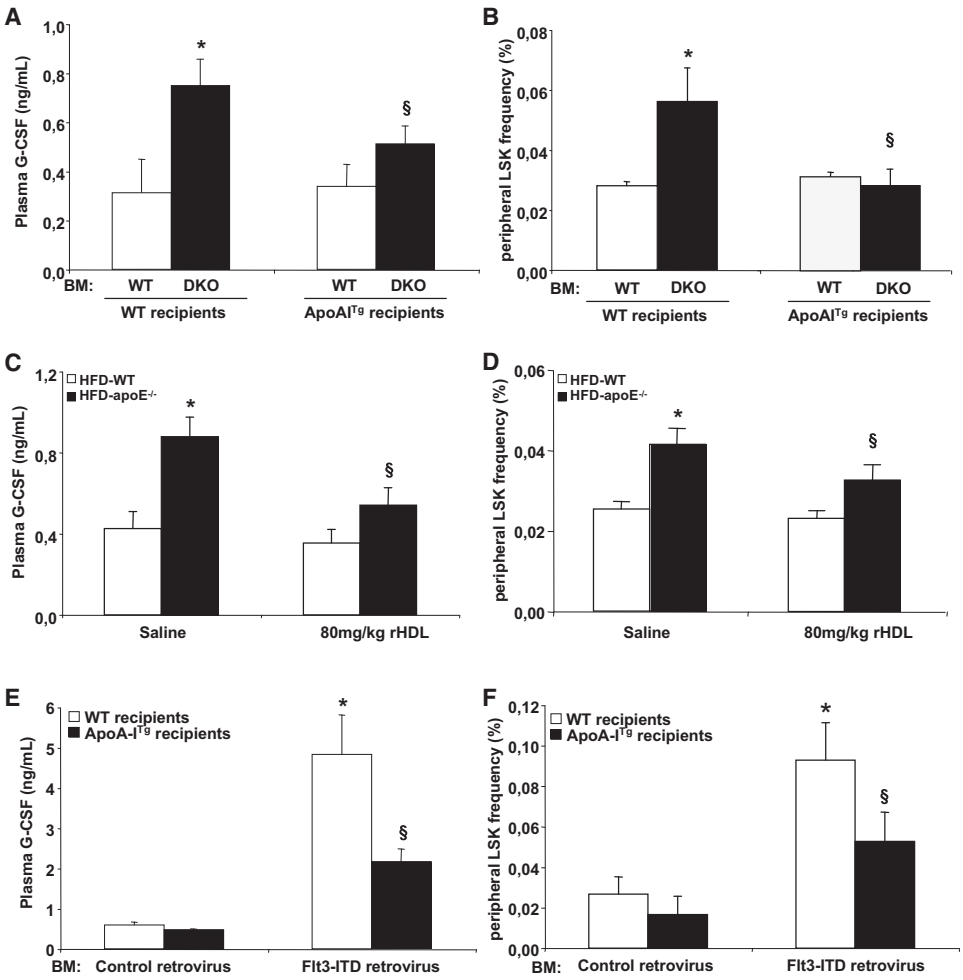

Figure 7. Raising HDL-Cholesterol Prevents HSPC Mobilization

Plasma G-CSF levels and quantification of circulating HSPCs by flow cytometry in WT and ApoA-I transgenic recipient mice transplanted with either WT or *Abca1*$^{-/-}$*Abcg1*$^{-/-}$ BM 12 weeks postreconstitution (A and B), in 4-week-old, high fat diet-fed WT and *apoE*$^{-/-}$ mice infused or not with 80 mg/kg rHDL for 96 hr (C and D), and in WT and ApoA-I transgenic recipient mice transplanted with BM transduced with retroviruses encoding the human oncogenic Flt3-ITD mutation 6 weeks postreconstitution (E and F) are shown. Results are ± SEM of four to six animals per group. *$p < 0.05$ versus WT. §$p < 0.05$, effect of HDL-raising treatment (hapoA-I^{Tg} or rHDL).

DISCUSSION

We have identified a role of cholesterol efflux pathways in limiting the mobilization of HSPCs and prevention of clinically detrimental extramedullary hematopoiesis in mouse models of myeloproliferative disorders. In mice with knockout of transporters ABCA1 and ABCG1 in all BM cells, or exclusively in macrophages or dendritic cells, increased IL-23-dependent production of growth factor G-CSF alters the BM niche leading to HSPC mobilization and infiltration of distant organs. Concordant with a recent study (Rieger et al., 2009), increased G-CSF acts via GMPs to direct myeloid production toward neutrophils rather than monocytes, eventuating in BM macrophage depletion. Consequently, OB populations as well as the production of SDF-1/Cxcl12 are reduced. Importantly, our findings indicate a beneficial effect of increased HDL levels in preventing or reversing HSPC mobilization and extramedullary hematopoiesis, not only in *Abca1*$^{-/-}$*Abcg1*$^{-/-}$ mice and *Apoe*$^{-/-}$ mice but also in a mouse model of hematological malignancy. These findings suggest a therapeutic application of rHDL infusion in the prevention of extramedullary hematopoiesis in both atherosclerosis and hematologic malignancies.

Ley and colleagues have defined a negative feedback loop controlling granulopoiesis in which uptake of apoptotic neutrophils by macrophages and dendritic cells leads to suppression of IL-23 production, decreased release of IL-17 by lymphocytes, and decreased production of G-CSF by bone marrow stromal cells (Stark et al., 2005). Our results provide evidence that activation of the IL-23/IL-17/G-CSF signaling axis in mice with defective cholesterol efflux pathways leads to increased HSPC mobilization. Moreover, by using cell-specific knockouts of ABCA1 and ABCG1, we show the importance of the cholesterol efflux pathways in macrophages and dendritic cells in the control of IL-23 production. This links the control of HSPC mobilization to cholesterol homeostasis in the innate immune system.

In agreement with previous studies (Rieger et al., 2009), increased plasma G-CSF levels in *Abca1*$^{-/-}$*Abcg1*$^{-/-}$ mice direct hematopoietic lineages in vitro toward neutrophil rather than monocyte/macrophage production. This led to an expansion of neutrophils and loss of macrophage populations in the BM. Neutrophil expansion in *Abca1*$^{-/-}$*Abcg1*$^{-/-}$ mice transformed the BM into a highly proteolytic environment (Lévesque et al., 2002) leading to cleavage of CXCR4 by neutrophil elastase 2 (Petit et al., 2002; Levesque et al., 2003). However, this alone could not explain enhanced HSPC mobilization because deletion of Elane or lentiviral overexpression of CXCR4 did not rescue this phenotype. Rather, our studies indicated an essential role of reduced BM SDF-1/Cxcl12 production in HSPC mobilization. This is consistent with the recently demonstrated role of decreased SDF-1/Cxcl12 in mediating the effect of G-CSF on HSPC mobilization (Levesque et al., 2004; Semerad et al., 2005; Christopher and Link, 2008).

While macrophage depletion has been shown to promote HSPC mobilization by disruption of the osteoblastic niche through impaired osteoblast (OB) activity and SDF-1/Cxcl12 production (Winkler et al., 2010; Gordy et al., 2011; Chow et al., 2011; Christopher et al., 2011), the link with endogenous plasma G-CSF appears to be unexplored. Greater endogenous plasma G-CSF induced the loss of BM macrophage populations in *Abca1*$^{-/-}$*Abcg1*$^{-/-}$ mice leading to decreased SDF-1/Cxcl12 production. This involved decreases in N-Cadherin^{+} OB subsets and Nestin^{+} progenitors. Previous studies have shown that these cell populations have a key role in maintaining HSPCs in their niche (Lymperi et al., 2008; Visnjic et al., 2004; Méndez-Ferrer et al., 2010; Raaijmakers et al., 2010). Thus, our study shows that cholesterol efflux pathways in splenic macrophages and dendritic cells are linked to control of the osteoblastic niche and HSPC mobilization via the IL23/IL17/G-CSF signaling axis.

Overexpression of the human apoA-I transgene to raise HDL levels prevented the myeloproliferative disorders of *Abca1*$^{-/-}$ *Abcg1*$^{-/-}$ BM transplanted mice (Yvan-Charvet et al., 2010). We now provide evidence that this effect was partly mediated by reduced plasma G-CSF levels and HSPC mobilization. We recently showed that *Apoe*$^{-/-}$ mice have expanded and proliferating HSPCs (Murphy et al., 2011). ApoE is expressed on the surface of HSPCs where it appears to interact with ABCA1 and ABCG1 to promote cholesterol efflux (Laffitte et al., 2001; Murphy et al., 2011). *Apoe*$^{-/-}$ mice also develop hepatosplenomegaly on WTDs likely reflecting extramedullary hematopoiesis (Murphy et al., 2011). A recent study has shown that the spleen represents an important reservoir of monocytes in *Apoe*$^{-/-}$ mice, contributing directly to atherosclerotic lesions (Robbins et al., 2012). Together with our study, this suggests that extramedullary hematopoiesis resulting from increased G-CSF in *Apoe*$^{-/-}$ mice plays a role in atherogenesis. Moreover, infusion of cholesterol-poor phospholipid/apoA-I complexes (i.e, rHDL; Murphy et al., 2011), suppressed plasma G-CSF levels and HSPC mobilization, uncovering a potential anti-atherogenic effect of this treatment.

The relevance of the human apoA-I transgene was also tested in a mouse model of myeloproliferative disorder induced by an activating mutation in the Flt3 gene (Flt3-ITD), the most common mutation associated with acute myeloid leukemia (AML) in humans. Consistent with their myeloproliferative disorder, mice that received BM transduced with retroviruses encoding Flt3-ITD exhibited splenomegaly (Kelly et al., 2002), and this was associated with increased splenic expression of IL-23, increased plasma G-CSF, and HSC mobilization, likely reflecting an underlying expansion of DCs by Flt3 signaling (Liu and Nussenzweig, 2010). The MPN was associated with reduced plasma cholesterol, and raising HDL levels though overexpression of the human apoA-I transgene partially prevented these defects. Our findings indicate that HDL-mediated cholesterol efflux pathways in macrophages and dendritic cells act to suppress HSPC mobilization and extramedullary hematopoiesis, and that HDL raising treatments could have beneficial effects on these processes in atherosclerosis and hematological malignancies.

EXPERIMENTAL PROCEDURES

Mice and Treatments

Human apoA-I transgenic (B6.Tg(ApoA1)$^{1Rub/J}$), *Apoe*$^{-/-}$ (B6.129P2-*Apoe*^{tm1Unc}), *Elane*$^{-/-}$ (B6.129X1-Elane$^{tm1Sds/J}$), Nestin-Cre (B6.Cg-Tg(nes-cre)$^{1kln/J}$), and Rosa^{EYFP} (B6.129x1Gt(Rosa)$^{26Sortm1EYFP/J}$) mice were obtained from the Jackson laboratory. Wild-type and *Abca1*$^{-/-}$*Abcg1*$^{-/-}$ littermates in a mixed C57BL/6 × DBA background (Yvan-Charvet et al., 2007) were used for this study, unless otherwise noted. *LysM-Cre Abca1*$^{fl/fl}$*Abcg1*$^{fl/fl}$ mice and *CD11c-Cre Abca1*$^{fl/fl}$*Abcg1*$^{fl/fl}$ mice were obtained by crossing *Abca1*$^{fl/fl}$ mice (kindly provided by Dr. Parks, Wake Forest University) and *Abcg1*$^{fl/fl}$ mice (generated at Columbia University) with *LysM-Cre* mice (B6.129P2-Lyz2$^{tm1(cre)Ifo/J}$) and *CD11c-Cre* mice (C57BL/6J-Tg(Itgax-cre,-EGFP)), respectively, from the Jackson laboratory. Cre efficiency was confirmed by RT-PCR against the targeted ABCA1 and ABCG1 genes in macrophages and dendritic cells, respectively (data not shown). Mice were fed either a regular chow diet or a Western diet (TD 88137, Harlan Teklad) as indicated in the figure legends. BM transplantation into the genetically uniform F1 generation obtained by crossing C57BL/6 wild-type or hapoA-1^{Tg} mice with wild-type DBA mice (The Jackson laboratory) was performed as previously described (Yvan-Charvet et al., 2007). For neutralizing antibody experiments, WT and *Abca1*$^{-/-}$*Abcg1*$^{-/-}$ BM transplanted mice were i.p. injected 16 hr before analysis with the following antibodies: anti-IL-3Rβ AF549, anti-Cxcl2 MAB452, anti-IL-23R MAB1686, anti-IL-17 MAB421, and anti-G-CSF MAB414 (all from R&D Systems). Treatments with rHDL (provided by CSL Australia) or vehicle (saline) were administered via the tail vein. All mice were housed at Columbia University Medical Center according to animal welfare guidelines. Mice were maintained on a 12 hr light/12 hr darkness lighting schedule. Animals had ad libitum access to both food and water.

Colony-Forming Assay

All experiments were performed between 12:00 and 1:00 p.m. to limit variability between experiments. For peripheral blood CFU assays, 300 μl of blood were collected into EDTA tubes before red blood cell lysis, filtration, and centrifugation for 5 min at 1,000 rpm. Splenocytes were extracted by pressing spleens through a stainless steel grid. Single-cell suspension was submitted to red blood cell lysis, filtration, and centrifugation for 5 min at 1,000 rpm. For liver, lung, and heart CFU assays, tissues were cut in small piece and digested with 1 mg/ml collagenase D (Roche) for 30 min at 37°C before red blood cell lysis, filtration, and centrifugation for 5 min at 1,000 rpm. Peripheral cells, splenocytes (5×10^4), liver, lung, and heart cells (1×10^6) were plated in methylcellulose-based media containing a cocktail of recombinant cytokines including SCF, IL-3, and IL-6 (Methocult, Stemcell) supplemented with 2% FCS to generate multipotential progenitor cells (CFU-GEMM) in presence or absence of 10% IL-3 supplement media (BD Bioscience) and GM-CSF (2 ng/ml) (Mix conditions) (R&D Systems) to generate granulocyte-macrophage progenitors (CFU-GMs). The number of CFUs per dish was scored after 10 days of differentiation.

Flow Cytometry Analysis and Cell Sorting

BM cells, peripheral blood leukocytes, and splenocytes were collected as described above. Cells were stained with the appropriate antibodies for

30 min on ice. Intracellular stainings were performed using the Cytofix/Cytoperm kit (BD Biosciences) according to the manufacturer's protocol. Endothelial cells, osteoblasts, and Nestin$^+$ cells were isolated at previously described (Semerad et al., 2005). Briefly, tibias and femurs were flushed thoroughly of BM cells, chopped with a scalpel, and washed three times to further remove residual BM cells. The bone fragments were then digested with collagenase type IA (Sigma-Aldrich) for 30 min at 37°C before red blood cell lysis, filtration, and centrifugation for 5 min at 1,000 rpm. Multiparameter analyses of stained cell suspensions were performed on a four-laser BD LSRII cell analyzer or sorted on a BD FACSAria Cell Sorter both running with DiVa software (BD Biosciences). Viable cells were gated by light scatter or exclusion of CD45$^-$ cells. Data were analyzed using FlowJo software (Tree Star Inc.).

Statistical Analysis

Statistical significance was assessed by performing two-tailed parametric Student's t test or one-way analysis of variance (ANOVA, four-group comparisons) with a Bonferroni multiple comparison post-test (GraphPad software, San Diego, CA).

SUPPLEMENTAL INFORMATION

Supplemental Information includes Supplemental Results, Supplemental Experimental Procedures, and seven figures and can be found with this article online at http://dx.doi.org/10.1016/j.stem.2012.04.024.

ACKNOWLEDGMENTS

We thank Dr. Kristie Gordon for assistance with flow cytometry, CSL Australia for providing the rHDL used in this study, and Dr. David W. Dempster for help on bone histomorphometry analysis. This work was supported by grants to L.Y.C. from the American Heart Association (SDG2160053), to M.W. from the Netherlands Organization of Scientific Research (NWO VENI 916.11.072), and to A.R.T. from the NIH (HL54591).

Received: December 8, 2011
Revised: March 20, 2012
Accepted: April 20, 2012
Published: August 2, 2012

REFERENCES

Chow, A., Lucas, D., Hidalgo, A., Méndez-Ferrer, S., Hashimoto, D., Scheiermann, C., Battista, M., Leboeuf, M., Prophete, C., van Rooijen, N., et al. (2011). Bone marrow CD169+ macrophages promote the retention of hematopoietic stem and progenitor cells in the mesenchymal stem cell niche. J. Exp. Med. *208*, 261–271.

Christopher, M.J., and Link, D.C. (2008). Granulocyte colony-stimulating factor induces osteoblast apoptosis and inhibits osteoblast differentiation. J. Bone Miner. Res. *23*, 1765–1774.

Christopher, M.J., Liu, F., Hilton, M.J., Long, F., and Link, D.C. (2009). Suppression of CXCL12 production by bone marrow osteoblasts is a common and critical pathway for cytokine-induced mobilization. Blood *114*, 1331–1339.

Christopher, M.J., Rao, M., Liu, F., Woloszynek, J.R., and Link, D.C. (2011). Expression of the G-CSF receptor in monocytic cells is sufficient to mediate hematopoietic progenitor mobilization by G-CSF in mice. J. Exp. Med. *208*, 251–260.

Dar, A., Goichberg, P., Shinder, V., Kalinkovich, A., Kollet, O., Netzer, N., Margalit, R., Zsak, M., Nagler, A., Hardan, I., et al. (2005). Chemokine receptor CXCR4-dependent internalization and resecretion of functional chemokine SDF-1 by bone marrow endothelial and stromal cells. Nat. Immunol. *6*, 1038–1046.

Dessì, S., Batetta, B., Spano, O., Sanna, F., Tonello, M., Giacchino, M., Tessitore, L., Costelli, P., Baccino, F.M., Madon, E., et al. (1995). Clinical remission is associated with restoration of normal high-density lipoprotein cholesterol levels in children with malignancies. Clin. Sci. *89*, 505–510.

Ehninger, A., and Trumpp, A. (2011). The bone marrow stem cell niche grows up: mesenchymal stem cells and macrophages move in. J. Exp. Med. *208*, 421–428.

Fibbe, W.E., Pruijt, J.F., Velders, G.A., Opdenakker, G., van Kooyk, Y., Figdor, C.G., and Willemze, R. (1999). Biology of IL-8-induced stem cell mobilization. Ann. N Y Acad. Sci. *872*, 71–82.

Fossiez, F., Djossou, O., Chomarat, P., Flores-Romo, L., Ait-Yahia, S., Maat, C., Pin, J.J., Garrone, P., Garcia, E., Saeland, S., et al. (1996). T cell interleukin-17 induces stromal cells to produce proinflammatory and hematopoietic cytokines. J. Exp. Med. *183*, 2593–2603.

Gilbert, H.S., Ginsberg, H., Fagerstrom, R., and Brown, W.V. (1981). Characterization of hypocholesterolemia in myeloproliferative disease. Relation to disease manifestations and activity. Am. J. Med. *71*, 595–602.

Gordy, C., Pua, H., Sempowski, G.D., and He, Y.W. (2011). Regulation of steady-state neutrophil homeostasis by macrophages. Blood *117*, 618–629.

Gourion-Arsiquaud, S., Allen, M.R., Burr, D.B., Vashishth, D., Tang, S.Y., and Boskey, A.L. (2010). Bisphosphonate treatment modifies canine bone mineral and matrix properties and their heterogeneity. Bone *46*, 666–672.

Greenbaum, A.M., and Link, D.C. (2011). Mechanisms of G-CSF-mediated hematopoietic stem and progenitor mobilization. Leukemia *25*, 211–217.

Guillaume, T., D'Hondt, V., and Symann, M. (1993). IL-3 and peripheral blood stem cell harvesting. Stem Cells *11*, 173–181.

Ivanov, I.I., Frutos, Rde.L., Manel, N., Yoshinaga, K., Rifkin, D.B., Sartor, R.B., Finlay, B.B., and Littman, D.R. (2008). Specific microbiota direct the differentiation of IL-17-producing T-helper cells in the mucosa of the small intestine. Cell Host Microbe *4*, 337–349.

Jaiswal, S., Jamieson, C.H., Pang, W.W., Park, C.Y., Chao, M.P., Majeti, R., Traver, D., van Rooijen, N., and Weissman, I.L. (2009). CD47 is upregulated on circulating hematopoietic stem cells and leukemia cells to avoid phagocytosis. Cell *138*, 271–285.

Kelly, L.M., Liu, Q., Kutok, J.L., Williams, I.R., Boulton, C.L., and Gilliland, D.G. (2002). FLT3 internal tandem duplication mutations associated with human acute myeloid leukemias induce myeloproliferative disease in a murine bone marrow transplant model. Blood *99*, 310–318.

Kiel, M.J., Radice, G.L., and Morrison, S.J. (2007). Lack of evidence that hematopoietic stem cells depend on N-cadherin-mediated adhesion to osteoblasts for their maintenance. Cell Stem Cell *1*, 204–217.

Kraus, M.D., Bartlett, N.L., Fleming, M.D., and Dorfman, D.M. (1998). Splenic pathology in myelodysplasia: a report of 13 cases with clinical correlation. Am. J. Surg. Pathol. *22*, 1255–1266.

Laffitte, B.A., Repa, J.J., Joseph, S.B., Wilpitz, D.C., Kast, H.R., Mangelsdorf, D.J., and Tontonoz, P. (2001). LXRs control lipid-inducible expression of the apolipoprotein E gene in macrophages and adipocytes. Proc. Natl. Acad. Sci. USA *98*, 507–512.

Lévesque, J.P., Hendy, J., Takamatsu, Y., Williams, B., Winkler, I.G., and Simmons, P.J. (2002). Mobilization by either cyclophosphamide or granulocyte colony-stimulating factor transforms the bone marrow into a highly proteolytic environment. Exp. Hematol. *30*, 440–449.

Levesque, J.P., Hendy, J., Takamatsu, Y., Simmons, P.J., and Bendall, L.J. (2003). Disruption of the CXCR4/CXCL12 chemotactic interaction during hematopoietic stem cell mobilization induced by GCSF or cyclophosphamide. J. Clin. Invest. *111*, 187–196.

Levesque, J.P., Liu, F., Simmons, P.J., Betsuyaku, T., Senior, R.M., Pham, C., and Link, D.C. (2004). Characterization of hematopoietic progenitor mobilization in protease-deficient mice. Blood *104*, 65–72.

Liu, K., and Nussenzweig, M.C. (2010). Origin and development of dendritic cells. Immunol. Rev. *234*, 45–54.

Liu, F., Poursine-Laurent, J., and Link, D.C. (2000). Expression of the G-CSF receptor on hematopoietic progenitor cells is not required for their mobilization by G-CSF. Blood *95*, 3025–3031.

Lymperi, S., Horwood, N., Marley, S., Gordon, M.Y., Cope, A.P., and Dazzi, F. (2008). Strontium can increase some osteoblasts without increasing hematopoietic stem cells. Blood *111*, 1173–1181.

Lymperi, S., Ferraro, F., and Scadden, D.T. (2010). The HSC niche concept has turned 31. Has our knowledge matured? Ann. N Y Acad. Sci. *1192*, 12–18.

Méndez-Ferrer, S., Michurina, T.V., Ferraro, F., Mazloom, A.R., Macarthur, B.D., Lira, S.A., Scadden, D.T., Ma'ayan, A., Enikolopov, G.N., and Frenette, P.S. (2010). Mesenchymal and haematopoietic stem cells form a unique bone marrow niche. Nature *466*, 829–834.

Metcalf, D. (2008). Hematopoietic cytokines. Blood *111*, 485–491.

Morrison, S.J., Wright, D.E., and Weissman, I.L. (1997). Cyclophosphamide/granulocyte colony-stimulating factor induces hematopoietic stem cells to proliferate prior to mobilization. Proc. Natl. Acad. Sci. USA *94*, 1908–1913.

Murphy, A.J., Akhtari, M., Tolani, S., Pagler, T., Bijl, N., Kuo, C.L., Wang, M., Sanson, M., Abramowicz, S., Welch, C., et al. (2011). ApoE regulates hematopoietic stem cell proliferation, monocytosis, and monocyte accumulation in atherosclerotic lesions in mice. J. Clin. Invest. *121*, 4138–4149.

O'Malley, D.P., Kim, Y.S., Perkins, S.L., Baldridge, L., Juliar, B.E., and Orazi, A. (2005). Morphologic and immunohistochemical evaluation of splenic hematopoietic proliferations in neoplastic and benign disorders. Mod. Pathol. *18*, 1550–1561.

Perry, J.M., and Li, L. (2007). Disrupting the stem cell niche: good seeds in bad soil. Cell *129*, 1045–1047.

Petit, I., Szyper-Kravitz, M., Nagler, A., Lahav, M., Peled, A., Habler, L., Ponomaryov, T., Taichman, R.S., Arenzana-Seisdedos, F., Fujii, N., et al. (2002). G-CSF induces stem cell mobilization by decreasing bone marrow SDF-1 and up-regulating CXCR4. Nat. Immunol. *3*, 687–694.

Raaijmakers, M.H., Mukherjee, S., Guo, S., Zhang, S., Kobayashi, T., Schoonmaker, J.A., Ebert, B.L., Al-Shahrour, F., Hasserjian, R.P., Scadden, E.O., et al. (2010). Bone progenitor dysfunction induces myelodysplasia and secondary leukaemia. Nature *464*, 852–857.

Rieger, M.A., Hoppe, P.S., Smejkal, B.M., Eitelhuber, A.C., and Schroeder, T. (2009). Hematopoietic cytokines can instruct lineage choice. Science *325*, 217–218.

Robbins, C.S., Chudnovskiy, A., Rauch, P.J., Figueiredo, J.L., Iwamoto, Y., Gorbatov, R., Etzrodt, M., Weber, G.F., Ueno, T., van Rooijen, N., et al. (2012). Extramedullary hematopoiesis generates Ly-6C(high) monocytes that infiltrate atherosclerotic lesions. Circulation *25*, 364–374.

Semerad, C.L., Christopher, M.J., Liu, F., Short, B., Simmons, P.J., Winkler, I., Levesque, J.P., Chappel, J., Ross, F.P., and Link, D.C. (2005). G-CSF potently inhibits osteoblast activity and CXCL12 mRNA expression in the bone marrow. Blood *106*, 3020–3027.

Stark, M.A., Huo, Y., Burcin, T.L., Morris, M.A., Olson, T.S., and Ley, K. (2005). Phagocytosis of apoptotic neutrophils regulates granulopoiesis via IL-23 and IL-17. Immunity *22*, 285–294.

Sugiyama, T., Kohara, H., Noda, M., and Nagasawa, T. (2006). Maintenance of the hematopoietic stem cell pool by CXCL12-CXCR4 chemokine signaling in bone marrow stromal cell niches. Immunity *25*, 977–988.

Visnjic, D., Kalajzic, Z., Rowe, D.W., Katavic, V., Lorenzo, J., and Aguila, H.L. (2004). Hematopoiesis is severely altered in mice with an induced osteoblast deficiency. Blood *103*, 3258–3264.

Wang, X., Collins, H.L., Ranalletta, M., Fuki, I.V., Billheimer, J.T., Rothblat, G.H., Tall, A.R., and Rader, D.J. (2007). Macrophage ABCA1 and ABCG1, but not SR-BI, promote macrophage reverse cholesterol transport in vivo. J. Clin. Invest. *117*, 2216–2224.

Winkler, I.G., Sims, N.A., Pettit, A.R., Barbier, V., Nowlan, B., Helwani, F., Poulton, I.J., van Rooijen, N., Alexander, K.A., Raggatt, L.J., and Lévesque, J.P. (2010). Bone marrow macrophages maintain hematopoietic stem cell (HSC) niches and their depletion mobilizes HSCs. Blood *116*, 4815–4828.

Yvan-Charvet, L., Ranalletta, M., Wang, N., Han, S., Terasaka, N., Li, R., Welch, C., and Tall, A.R. (2007). Combined deficiency of ABCA1 and ABCG1 promotes foam cell accumulation and accelerates atherosclerosis in mice. J. Clin. Invest. *117*, 3900–3908.

Yvan-Charvet, L., Welch, C., Pagler, T.A., Ranalletta, M., Lamkanfi, M., Han, S., Ishibashi, M., Li, R., Wang, N., and Tall, A.R. (2008). Increased inflammatory gene expression in ABC transporter-deficient macrophages: free cholesterol accumulation, increased signaling via toll-like receptors, and neutrophil infiltration of atherosclerotic lesions. Circulation *118*, 1837–1847.

Yvan-Charvet, L., Pagler, T., Gautier, E.L., Avagyan, S., Siry, R.L., Han, S., Welch, C.L., Wang, N., Randolph, G.J., Snoeck, H.W., and Tall, A.R. (2010). ATP-binding cassette transporters and HDL suppress hematopoietic stem cell proliferation. Science *328*, 1689–1693.

Zhang, J., Niu, C., Ye, L., Huang, H., He, X., Tong, W.G., Ross, J., Haug, J., Johnson, T., Feng, J.Q., et al. (2003). Identification of the haematopoietic stem cell niche and control of the niche size. Nature *425*, 836–841.

Zhu, J., and Emerson, S.G. (2002). Hematopoietic cytokines, transcription factors and lineage commitment. Oncogene *21*, 3295–3313.